Dynamical footprints of Hurricanes in the Tropical Dynamics

Davide Faranda, Gabriele Messori, Pascal Yiou, Soulivanh Thao, Flavio Pons, Berengere Dubrulle

Dynamical footprints of Hurricanes in the Tropical Dynamics

D. Faranda,[1,2,3,a)] G. Messori,[4,5] P. Yiou,[1] S. Thao,[1] F. Pons,[1] and B. Dubrulle[6]

[1)]*Laboratoire des Sciences du Climat et de l'Environnement, UMR 8212 CEA-CNRS-UVSQ, Université Paris-Saclay & IPSL, CE Saclay l'Orme des Merisiers, 91191, Gif-sur-Yvette, France*

[2)]*London Mathematical Laboratory, 8 Margravine Gardens, London, W6 8RH, UK*

[3)]*LMD/IPSL, Ecole Normale Superieure, PSL research University, 75005, Paris, France*

[4)]*Department of Earth Sciences and Centre of Natural Hazards and Disaster Science (CNDS), Uppsala University, Uppsala, 75237, Sweden*

[5)]*Department of Meteorology and Bolin Centre for Climate Research, Stockholm University, Stockholm, 11418 Sweden.*

[6)]*SPEC, CEA, CNRS, Université Paris-Saclay, F-91191 CEA Saclay, Gif-sur-Yvette, France.*

(Dated: 10 November 2022)

Hurricanes — and more broadly tropical cyclones — are high-impact weather phenomena whose adverse socio-economic and ecosystem impacts affect a considerable part of the global population. Despite our reasonably robust meteorological understanding of tropical cyclones, we still face outstanding challenges for their numerical simulations. Consequently, future changes in the frequency of occurrence and intensity of tropical cyclones are still debated. Here, we diagnose possible reasons for the poor representation of tropical cyclones in numerical models, by considering the cyclones as chaotic dynamical systems. We follow 197 tropical cyclones which occurred between 2010 and 2020 in the North Atlantic using the HURDAT2 and ERA5 datasets. We measure the cyclones instantaneous number of active degrees of freedom (local dimension) and the persistence of their sea-level pressure and potential vorticity fields. During the most intense phases of the cyclones, and specifically when cyclones reach hurricane strength, there is a collapse of degrees of freedom and an increase in persistence. The large dependence of hurricanes dynamical characteristics on intensity suggests the need for adaptive parametrisation schemes which take into account the dependence of the cyclone's phase, in analogy with high-dissipation intermittent events in turbulent flows.

[a)]Correspondence to davide.faranda@lsce.ipsl.fr

I. LEAD PARAGRAPH

Tropical cyclones are both high-impact weather events and challenging phenomena from the point of view of numerical modelling. While their lifecycle is relatively well understood, there are still difficulties in the representation of their dynamics in weather and climate models, and in drawing robust conclusions on how different climate conditions may affect their frequency of occurrence and intensity. Here, we consider tropical cyclones as chaotic dynamical systems. We show that the formation of particularly intense cyclones, termed hurricanes in the North Atlantic, coincides with a reduction of the phase space of the atmospheric dynamics to a low-dimensional and persistent object, where few rotational kinetic degrees of freedom dominate the dynamics. This suggests the need for adaptive parameterisations to integrate the governing equations when simulating intense tropical cyclones in numerical climate models.

II. INTRODUCTION

Tropical cyclones are high-impact extreme weather events. For example, they are the costliest natural disaster category in the United States[1,2], with the damage related to hurricane Katrina (2005) alone amounting to about 1% of the gross domestic product of the country[2]. Trends in the frequency of occurrence and intensity of tropical cyclones are difficult to discern in observations because of their relative rarity and of the brevity of highly spatially and temporally resolved datasets, which rely on satellite observations[3]. Projections of future climates indicate an increase in the intensity of tropical cyclones in the North Atlantic sector, albeit only with medium confidence[4]. Indeed, reproducing the dynamics of the most severe events is difficult even in the most advanced global or regional climate models[5]. For example, while mid-latitude synoptic dynamics mostly originate from the chaotic structure of the motions associated with baroclinic instability[6,7], tropical cyclones are characterized by a rapid organization of convectively unstable flows whose dynamics is turbulent and highly sensitive to boundary conditions[8]. To understand the reasons for the poor representation of tropical cyclones in numerical models, we adopt a dynamical system methodology which represents the cyclones as states of a chaotic, high-dimensional system. We specifically compute two metrics reflecting instantaneous properties of the cyclones, namely persistence and local dimension. Local dimension is a proxy for the system's number of active

degrees of freedom, and can be linked to the system's predictability[9–11]. Persistence provides information about the dominant time scale of the dynamics. Both metrics may easily be applied to large datasets, such as climate reanalyses. They have recently provided insights on a number of geophysical phenomena, including transitions between transient metastable states of the mid-latitude atmosphere[9,12], palaeoclimate attractors[13,14], slow earthquake dynamics[15] and changes in mid-latitude atmospheric predictability under global warming[16].

All these applications have taken an Eulerian point-of-view, focusing on a fixed spatio-temporal domain. Here, we provide the first application of the two metrics from a (semi)-Lagrangian perspective, by computing the persistence and local dimension of tropical cyclones which we track in space and time. This approach is particularly suited to study the complex behavior of convectively unstable flow systems (see, e.g., [17] and chapter 12 in[18]). After putting the tropical cyclones in the dynamical system framework, we may investigate whether they act as generic points of the phase space or whether their dynamics exhibits a peculiar behavior. In the first case,the numerical parametrizations developed for generic tropical climate states should work well when applied to small-scale features of tropical cyclones. In the second case, cyclones dynamical properties are dependent on their intensity or dynamical phase (tropical,subtropical, extratropical). This suggests that leading parametrizations designed for generic tropical confection will not work properly when cyclones are present in a domain.

In the rest of the study, we compute the persistence and local dimension of tropical cyclones, and use these to outline a strategy to improve their numerical simulation.

III. OBSERVABLES FOR CYCLONE DYNAMICS

The historical cyclone data are the "best track data" from the Atlantic HURDAT2 database[19], developed by the National Hurricane Center. This database provides, amongst other variables, the location of tropical cyclones, their maximum winds, central pressure and categorisation. The values are obtained as a post-storm analysis of all available data, collected both remotely and in-situ. We specifically consider separately hurricanes (HU), tropical storms (TS) and post-tropical cyclones associated with an extratropical transition (EX). We further use instantaneous potential vorticity (PV) at 500 hPa and sea-level pressure (SLP) data from ECMWF's ERA5 reanalysis[20]. For both datasets we make use of 6-hourly data, and additionally data at the time when the HURDAT2 database displays a cyclone landfall; the ERA5 data is retrieved at a horizontal resolution

of 0.25°.

Our analysis includes all tropical cyclones classified in HURDAT2 from 2010 to 2020 included. We use semi-Lagrangian observables, i.e. we select a horizontal domain around the tropical cycloe location, of size $\sim$1200 $\times$ 1200 km (41 $\times$ 41 grid points in ERA5). The choice of SLP is motivated by its widespread use in hurricane tracking[21] and the fact that it is a first approximation of the horizontal velocity streamfunction. The PV is often used in the study of tropical cyclones and relates to their intensification and symmetry structure[22,23], and takes explicitly into account the strength of the cyclones warm core. Indeed, PV may be viewed as a metric of latent heat release and therefore of the intensity of the diabatic processes taking place in the tropical cyclones (cloud formation, precipitation) [24,25]. We specifically select mid-level PV, following for example[26,27]. As control parameter, we chose the maximum winds from HURDAT2, since this quantity can be directly connected to the economic loss caused by tropical cyclones[28].

IV. A DYNAMICAL SYSTEMS VIEW OF TROPICAL CYCLONES

We follow tropical cyclones in phase space as states of a chaotic, high-dimensional dynamical system. Each instantaneous state of the cyclone, as represented by a given atmospheric variable, corresponds to a point in a reduced phase space (namely a special Poincaré section). We sample these states at discrete points i, determined by the temporal resolution of the HURDAT2 data, that is every 6h or whenever the HURDAT2 database displays a cyclone landfall. Our aim is to diagnose the dynamical properties of the instantaneous (in time) and local (in phase-space) states of the cyclone, as represented by the chosen atmospheric variable and geographical domain (physical space in Fig. 1). To do so, we leverage two metrics issuing from the combination of extreme value theory with Poincaré recurrences[29–31]. We consider the ensemble $\{X_i\}$, which in our analysis are SLP or PV maps of all timesteps i for all tropical cyclones in our dataset, always centred on the cyclones location. We further consider a state of interest ζ, which would correspond to a single SLP or PV map drawn from this dataset. We then define logarithmic returns as:

$$g(X_i, \zeta) = -\log[\mathrm{dist}(X_i, \zeta)] \tag{1}$$

Here, "dist" is the Euclidean distance between pairs of SLP or PV maps, but more generally it can be any distance function between two vectors which tends to zero as the two vectors increasingly resemble each other. We thus have a time series g of logarithmic returns which is large at

times i when X_i is close to ζ.

We next define exceedances as $\{u(\zeta) = g(X_i,\zeta) - s(q,\zeta)\ \forall i :\ g(X_i,\zeta) > s(q,\zeta)\}$, where $s(q,\zeta)$ is a high threshold corresponding to the qth quantile of $g(X_i,\zeta)$. These are effectively the previously-mentioned Poincaré recurrences, for the chosen state ζ (phase space in Fig. 1). The Freitas-Freitas-Todd theorem[29,30] states that the cumulative probability distribution $F(u(\zeta))$ is approximated by the exponential member of the Generalised Pareto Distribution. We thus have that:

$$F(u,\zeta) \simeq \exp\left[-\vartheta(\zeta)\frac{u(\zeta)}{\sigma(\zeta)}\right] \tag{2}$$

The parameters u, namely the exceedances, and σ, namely the scale parameter of the Generalised Pareto Distribution, depend on the chosen state ζ, while ϑ is the so-called extremal index, namely a measure of clustering[32]. We estimate it here using the Süveges Estimator[33].

From the above, we can define two dynamical systems metrics: local dimension (d) and persistence (θ^{-1}). The local dimension is given by $d(\zeta) = 1/\sigma(\zeta)$, with $0 < d \leq +\infty$. When X_i contains all the variables of the system, the estimation of d based on extreme value theory has a number of advantages over traditional methods (e.g. the box counting algorithm[34]). First, it does not require to estimate the volume of different sets at different scales: the selection of $s(q)$ based on the quantile provides a selection of different thresholds s which depends on the recurrence rate around the point ζ. Moreover, it does not require the a-priori selection of the maximum embedding dimension, as the observable g is always a univariate time-series. Even when X_i does not contain all variables of the system, the estimation of d through extreme value theory is still a powerful tool to compare different states of high-dimensional chaotic systems[35].

The persistence of the state ζ is measured via the extremal index $0 < \vartheta(\zeta) < 1$. We define the inverse of the average residence time of trajectories around ζ as: $\theta(\zeta) = \vartheta(\zeta)/\Delta t$, with Δt being the timestep of the underlying data (here 6 hours). Since the extremal index is non-dimensional, $\theta(\zeta)$ has units of frequency. θ^{-1} is then a measure of persistence. If ζ is a fixed point of the attractor $\theta(\zeta) = 0$. For a trajectory that leaves the neighborhood of ζ at the next time iteration, $\theta = 1$. A caveat of our approach is that our dataset is constructed from a sequence of cyclones which is not continuous in space-time. This may introduce a bias in our calculation of θ if the final state of a cyclone is a recurrence of the initial state of the following cyclone. This is highly unlikely due to the very different nature of the growth versus weakening stages of tropical cyclones. We further note that this does not affect the computation of d, which is insensitive to time reshuffling.

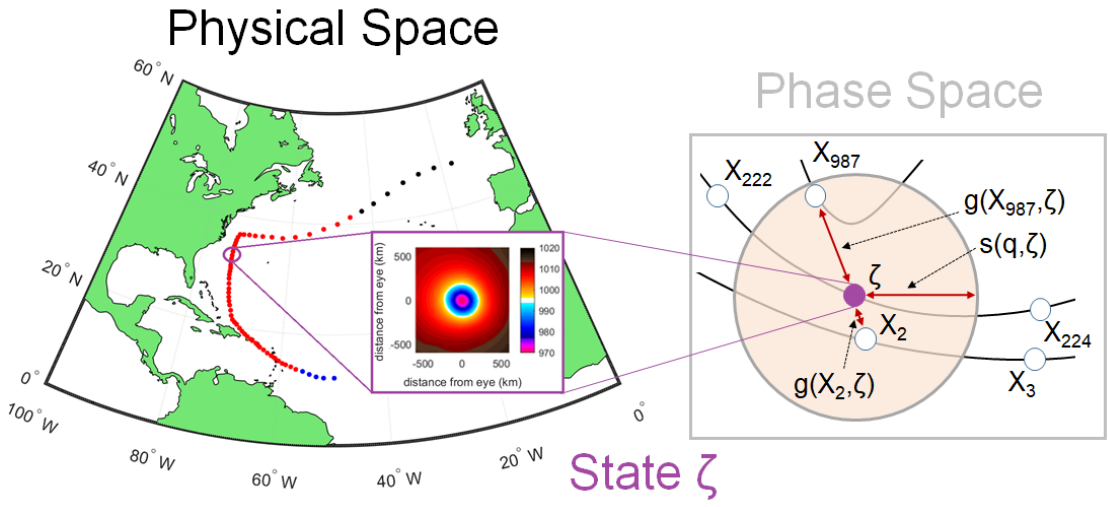

FIG. 1. Schematic of the computation of the dynamical systems metrics for an instantaneous state of a tropical cyclone. We take a snapshot of the cyclone in physical space (black quadrant), in this example a latitude-longitude map of sea-level pressure, which corresponds to state ζ in our reduced phase space. The right hand side panel shows the discrete sampling of the phase-space at points X_i (white circles). The shaded circle is a 2D representation of the hyper-sphere determined by the high threshold $s(q,\zeta)$, which defines recurrences. The logarithmic distances between measurements defined by $g(X_i,\zeta)$ are marked by double-headed arrows. For all points within the hyper-sphere, $g(X_i,\zeta) > s(q,\zeta)$ holds. In the schematic, only two measurements satisfy this condition (adapted from[14]).

While the derivation of d and θ^{-1} may seem very abstract, the two metrics can be related to the properties of the tropical cyclones. d is a proxy for the active number of degrees of freedom of the cyclones instantaneous states. On the other hand, θ^{-1} measures the persistence of such states and is related to the dominant time scale of the dynamics (the Lyapunov exponent[36]). Both these quantities are known to be connected to the dynamical (Kolmogorov Sinai) entropy since the seminal work of Young[37].

V. DYNAMICAL PROPERTIES OF TROPICAL CYCLONES: COLLAPSE OF DEGREES OF FREEDOM AND INCREASE IN PERSISTENCE IN INTENSE STORMS

Before focusing on the analysis of the dynamics of tropical cyclones specifically, we assess the peculiarity of their dynamical footprints when compared with a box of the tropical Atlantic

ocean. We use ERA5 6h data for SLP and PV covering the period 2017-2021 and considered the squared horizontal domain spanning 10N<Latitude<20N -50W<Longitude<40W. This region is chosen because it is located in an area where there are tropical features (such as disorganized and organized convection, tropical waves, ...) but not strong trade winds, that is synoptic structures are not advected either to the east or to the west. These latitudes were mostly avoided by the traders in their trips to the Americas because of the absence of winds[38]. We disregarded the choice of other tropical regions as they may be affected by stronger trade winds, or may include a wrong proportion of sub-tropical or extra-tropical features.

The results are shown in Figure 2. For SLP (Fig. 2a), that is the non cyclonic states do not feature any particular structure and they are characterized by non-persistent behavior ($\theta \lessapprox 1$) and a range of dimensions similar to those of the tropical cyclones. For PV, at a first glance, there is no clear separation between control box and tropical cyclones of the distributions on the basis of the analysis of the diagrams (Fig. 2b) with d and θ spanning a similar range of values. On the other hand, the analysis of the violin plots presented in Fig. 2c-f) show that the distributions are different. To quantify this difference we apply a two-sided Cramer-von Mises test at the 0.05 significance level[39]. The p-values found (virtually 0) imply that the null hypothesis that the two samples come from the same distribution can be rejected hinting to a statistically significant difference.

The previous analysis shows that the distribution of dynamical properties of tropical cyclones is significantly different from the one of a control box of the tropical Atlantic ocean. However, a fixed box control experiment, although in a region without strong average mean flow, is different from a region which moves following cyclones centers. The HURDAT2 database used in this study divides cyclones timesteps in different categories which span tropical, subtropical and extra-tropical objects with different intensities. The first step to understand whether the dynamical indicators exhibit a dependence on cyclone intensities is therefore to compute averages of d and θ conditioned to HURDAT2 cyclones status. Results are shown in Table 1. For tropical (pink) cyclones status, we remark a monotonic decrease of the average d_{SLP} and θ_{SLP} from the intensity, supporting the idea that intense cyclones yield low dimensional and persistent states of the dynamics when tracked by SLP observable. When looking at 500 hPa PV dynamical indicators, there is a non-monotonic relationship between intensity and d_{PV} while θ_{PV} increases monotononically with the intensity. For subtropical or extratropical cyclone status (turquoise in Table 1) we obtain similar results as tropical status for d_{SLP}, θ_{SLP} and θ_{PV} while d_{PV} monotonically increases. Finally we also report for completeness the other categories included in HURDAT2 in Table 1

(mustard) including Disturbances and Non-tropical lows. This first analysis suggests that there is a dependence of the dynamical indicators from cyclones intensities and type.

To go more in depth, Figure 3a, b shows the values of dimension d and inverse persistence θ computed on SLP and 500 hPa PV, with maximum winds in colours. The two local dimensions show different ranges, with $d_{SLP} < 30$ and d_{PV} attaining higher values. This reflects the fact that the PV dynamics involve multiple spatial scales, which reflect several underlying phenomena coming from convective and larger-scale aspects of cyclones and tropical dynamics, e.g. atmospheric waves[40]. SLP, on the other hand, reflects the synoptic-scale structures ($\sim 10^3$ km). The range of local dimensions found is relatively low compared to the number of grid-points used, which is 41 $\times$ 41. This means that the majority of the degrees of freedom are frozen when we follow coherent convective phenomena such as tropical cyclones. Moreover, lag-0 cross correlation coefficient between d_{SLP} and d_{PV} is 0.23, suggesting that the two variables carry different information. The persistence range is also different for SLP and PV, with $0.1 < \theta_{SLP} < 1$ and $0.3 < \theta_{PV} < 0.8$. In units of time, these values indicate an SLP persistence between 6 and 60 hours and a PV persistence between 7.5 and 20 hours. A timescale of 1–2.5 days is consistent with the synoptic-scale intensification of a cyclone, while timescales of a few hours to a day are consistent with changes in the convective structure of a cyclone. The lag-0 cross correlation coefficient coefficient between θ_{SLP} and θ_{PV} is 0.02, even lower than for d, again suggesting that the two carry different information.

We now connect the values of d and θ for SLP and PV to the underlying physics of the storms using the maximum wind speed. For SLP (Figure 3a) we note a strong dependence of θ on the maximum winds. Low to moderate winds are associated with high θ, while stronger winds correspond to lower θ. A weaker relation holds for d_{SLP} and maximum winds. For PV (Figure 3b), strong winds match low d values and intermediate-to-high θ values. Thus, SLP suggests that intense cyclones correspond to persistent states, while PV that they display a low local dimension and intermediate-to-low persistence. Looking at the scatterplots and PDFs of the two dynamical systems metrics conditioned on the HURDAT2 cyclone classification (Figure 3c, d), provides a picture consistent with the above. For SLP, HU and EX display a markedly higher persistence than TS. For PV, HU display a lower dimension and lower persistence than both TS and EX. The medians of all PDFs are significantly different at the 1% level under a Wilkoxon rank sum test, except for d_{SLP} for HU and EX (not shown). We interpret these dynamical system properties

Hurdat Entry	Short Description	d_{SLP}	θ_{SLP}	d_{PV}	θ_{PV}
	Control Box	5.4±1.5	0.98±0.02	17±9	0.48±0.07
WV	Tropical Waves	7.4±2.2	0.87±0.07	14±5	0.47±0.06
TD	Tropical Depressions (<34 kts)	6.3±3	0.76±0.16	19±7	0.49±0.08
TS	Tropical Storms (34-63 kts)	6.1±2.3	0.7±0.17	19±7	0.53±0.08
HU	Hurricanes (>64 kts)	5.6±1.8	0.51±0.19	14±5	0.55±0.08
SD	Subtropical Depressions (<34 kts)	6.2±1.8	0.64±0.18	17±8	0.43±0.07
SS	Subtropical Storms (>34 kts)	5.7±1.3	0.54±0.15	19±6	0.47±0.07
EX	Extratropical Cyclones	5.8±2.2	0.43±0.18	22±7	0.50±0.08
DB	Disturbances	5.5±1.9	0.70±0.15	18±9	0.48±0.08
LO	Non-tropical Lows	5.9±2.6	0.71±0.19	18±7	0.46±0.07

TABLE I. Average values of the dynamical indicators per class of HURDAT2 entries and for the control box. The error is given in terms of one standard deviation of the mean. Pink: tropical synoptic objects, turquoise: subtropical or extratropical objects, moustard: none of the previous categories, fluo green: control box values.

as follows. When the storms produce strong winds and diabatic phenomena (HU with high PV values and strong precipitation), the convective-scale dynamics collapses to an object with few degrees of freedom (low d_{PV}), yet low persistence (high θ_{PV}). Nonetheless, the synoptic-scale HU field is highly persistent (low θ_{SLP}), with values comparable to those of EX. SLP reflects a quasi-symmetrical horizontal cyclonic structure, which for both HU and EX is characteristic of the cyclone over an extended period of time. Weaker TS likely do not have a coherent cyclonic core throughout their life cycle, as reflected in the high values of θ_{SLP}.

The mean SLP and PV footprints of the system are qualitatively similar across all three cyclone categories (Fig. 4), although EX show a larger spatial scale than both TS and HU. In all three cases, the structures are roughly axisymmetric, showing that the EX cyclones included in HURDAT2 still retain tropical-like characteristics. Clearer differences emerge when looking at the standard deviation of the SLP and PV maps, computed at each gridpoint over all maps included in our analysis (Fig. 5). Here, HU and TS show qualitatively similar, axisymmetric structures, while EX show a clear meridional asymmetry in SLP and a less marked zonal asymmetry in PV. Notwithstanding the broad similarity in mean structure between three cyclone categories, the dy-

namical systems metrics are nonetheless able to differentiate their characteristics. This suggests that they sample from the systems dynamic variability and other subtle differences that do not emerge from the composite maps, such as the evolution of the system mean structure during the different phases of its lifecycle.

VI. DYNAMICAL SYSTEMS METRICS AND RAPID INTENSIFICATION

We now investigate whether the same dynamical systems framework can be used to investigate rapid intensification. Rapid intensification occurs when a tropical cyclone gains strength dramatically in a short period of time[41]. This phenomenon, difficult to explain from a theoretical point of view[42,43], results in an enhancement of the destructiveness potential of the cyclone and in a lower predictability of its trajectory[44]. Rapid intensification is usually quantified using the increment Δv of maximum winds over 24h. According to this definition, a cyclone is rapidly intensifying (resp. weakening) when $\Delta v > 35$ kts (resp. $\Delta v < -35$ kts). In phase space, rapid changes of the dynamics correspond to approaching unstable regions of the attractor[45,46]. Our working hypothesis is that variations in the dynamical systems metrics may be able to track these transitions. Figures 6 and 7 show the values of (a) Δd and (b) $\Delta\theta$ associated with the rapid intensification or weakening of the cyclones. The Δ are again computed over a period of 24 hours. Lateral panels show the PDFs of Δd and (b) $\Delta\theta$ conditioned on the rapid weakening or intensification. In both Figures 6 and 7 the medians of all PDFs for rapid weakening or intensification are significantly different at the 1% level under a Wilkoxon rank sum test, except for $\Delta\theta_{PV}$. Rapid intensification is associated with a clear decrease of θ_{SLP} and a weak decrease of d_{PV}. In other words, there is a large coherence of the dynamics of the cyclones tracked by the increased persistence of the SLP. This is accompanied by a decrease of the degrees of freedom in PV. The rapid weakening displays instead a decreased SLP persistence and a marked increase in d_{PV}.

VII. IMPLICATIONS OF THE RESULTS FOR THE NUMERICAL SIMULATION OF HURRICANES

We now discuss our results in the framework of the dynamical systems theory established for the indicators of persistence and dimensionality. From this viewpoint, high persistence and low

dimensional states are found at unstable fixed points of the dynamics. The link between unstable fixed points and persistence has been established in theorem 4.2.7 in[31]. The theorem states that the extremal index θ is smaller than 1 at periodic points and that its value depends on the degree of periodicity. The physical implication of the theorem is that the more stable the state, the closer the value of θ to 0. The limiting case, $\theta = 0$ corresponds to an infinite cluster length, that is the dynamics never leave the state, namely an equilibrium fixed point. If instead the value is close to 0 but not zero, the system sticks around the state for a long time, but it will eventually leave. This is a property of fixed points that have at least one unstable direction through which the system can leave the neighborhood. There is no formal theorem on the connection between a low dimension and fixed points, but an argument based on synchronization in[35]. In this study the local dimension is computed for spatially extended systems: Coupled Lattice Maps (CLMs). These dynamical systems are characterized by a coupling by adjacent sites. In the limit for extreme coupling, the CLMs have a fixed point where all the dynamics is synchronized and $d = 1$ (one particle is in the state of all the others). In real systems where perfect coupling does not exist, the states of low dimension d also correspond to synchronized states. For both the cases, to the best of our knowledge, it has not been proved that having a low θ and d is a sufficient condition for unstable fixed points. Furthermore the phase space that we use in our study is rather unusual: i) we do not consider the full set of variables but only two observables that project the dynamics of the cyclones on a special low dimensional subset, ii) the domain is moving and it is centered on the eye of the storm; yet it is not a Lagrangian phase space, because we only follow the eye and not each single fluid parcel.

Besides the exact mathematical meaning of our results, they are useful to highlight some practical aspects related to the simulation of these objects in climate and weather models. The large spread of the dynamical properties obtained in tropical cyclones and the strong dependency on the intensity suggests that a parametrization independent on cyclone intensity may fail to resolve their dynamics, especially for intense cyclones. Parameterizations are devised for typical states of tropical dynamics (isolated thunderstorms), but not specifically for the organized states of the most intense tropical cyclones. Hurricanes, i.e. intense tropical cycones, would then be analogous to dissipative singularities of turbulent flows[47], or *black holes* of the atmospheric dynamics[48]. In these cases, the physics is far from that of the average states of the system, such that adaptive scaling laws and targeted parametrizations are needed. Thus, the computation of the dynamical systems metrics could support the development of hurricane-specific parameterizations.

As a caveat, we underline that our semi-Lagrangian approach does not allow to relate the present results to the predictability of the trajectories of the tropical cyclones examined in this study, unlike the Eulerian approach applied to extra-tropical motions in [9–11]. Furthermore, we have used the ERA5 dataset, which has a fair but not highly-resolved representation of the convective scales of hurricane dynamics.

To conclude, we have shown that the physical characteristics of tropical cyclones may be understood in terms of dynamical systems metrics, which are capable of singling out peculiar states of the dynamics. Our results support the idea that cyclones can be understood as being reached along specific directions of the dynamics, consistent with instanton theory[49] and the notion of melancholia states[50]. This perspective opens intriguing possibilities, including the use of importance sampling algorithms[51] to select simulations which approach the hurricanes states as detected from the dimension–persistence analysis in the phase space. For example, in[52] we propose a methodology, based on dimension and persistence metrics, to reconstruct the statistics of cyclone intensities in coarse-resolution datasets, where maximum wind speed and minimum sea-level pressure may not be accurately represented. We conclude that the dynamical systems metrics outlined here could help to address several open problems in representing the climatology of cyclone dynamics and provide strategies for their parametrization and their characterization in climate simulations.

VIII. ACKNOWLEDGMENTS

The authors acknowledge Jacopo Riboldi, Valerio Lucarini, two anonymous reviewers and the editorial board for useful comments. DF acknowledge the support of the INSU-CNRS-LEFE-MANU grant (project DINCLIC), the grant ANR-19-ERC7-0003 (BOREAS), and grant ANR-20-CE01-0008-01 (SAMPRACE). This work has received support from the European Union's Horizon 2020 research and innovation programme (Grant agreement No. 101003469, XAIDA) and from the European Research Council (ERC) under the European Union's Horizon 2020 research and innovation programme (Grant agreement No. 948309, CENÆ project). B. Dubrulle was partly supported by the ANR, project EXPLOIT (grant agreement No. ANR-16-CE06-0006-01).

IX. DATA AVAILABILITY

ERA5 data are available on the C3S Climate Data Store on regular latitude-longitude grids at 0.25° x 0.25° resolution at `https://cds.climate.copernicus.eu/#!/home`, accessed on 2022-02-23

HURDAT2 is a database provided by NOAA and freely available at `https://www.aoml.noaa.gov/hrd/hurdat/Data_Storm.html`, accessed on 2022-02-23

REFERENCES

[1]A. B. Smith and R. W. Katz, "Us billion-dollar weather and climate disasters: data sources, trends, accuracy and biases," Natural hazards **67**, 387–410 (2013).

[2]A. Grinsted, P. Ditlevsen, and J. H. Christensen, "Normalized us hurricane damage estimates using area of total destruction, 1900- 2018," Proceedings of the National Academy of Sciences **116**, 23942–23946 (2019).

[3]E. K. Chang and Y. Guo, "Is the number of north atlantic tropical cyclones significantly underestimated prior to the availability of satellite observations?" Geophysical Research Letters **34** (2007).

[4]J. Kossin, T. Hall, T. Knutson, K. Kunkel, R. Trapp, D. Waliser, and M. Wehner, "Extreme storms," (2017).

[5]M. J. Roberts, J. Camp, J. Seddon, P. L. Vidale, K. Hodges, B. Vannière, J. Mecking, R. Haarsma, A. Bellucci, E. Scoccimarro, *et al.*, "Projected future changes in tropical cyclones using the cmip6 highresmip multimodel ensemble," Geophysical Research Letters **47**, e2020GL088662 (2020).

[6]E. N. Lorenz, "Can chaos and intransitivity lead to interannual variability?" Tellus A **42**, 378–389 (1990).

[7]S. Schubert and V. Lucarini, "Covariant lyapunov vectors of a quasi-geostrophic baroclinic model: analysis of instabilities and feedbacks," Quarterly Journal of the Royal Meteorological Society **141**, 3040–3055 (2015).

[8]C. J. Muller and D. M. Romps, "Acceleration of tropical cyclogenesis by self-aggregation feedbacks," Proceedings of the National Academy of Sciences **115**, 2930–2935 (2018).

[9]D. Faranda, G. Messori, and P. Yiou, "Dynamical proxies of north atlantic predictability and extremes," Scientific reports **7**, 41278 (2017).

[10]G. Messori, R. Caballero, and D. Faranda, "A dynamical systems approach to studying midlatitude weather extremes," Geophysical Research Letters **44**, 3346–3354 (2017).

[11]A. Hochman, P. Alpert, T. Harpaz, H. Saaroni, and G. Messori, "A new dynamical systems perspective on atmospheric predictability: Eastern mediterranean weather regimes as a case study," Science advances **5**, eaau0936 (2019).

[12]A. Hochman, G. Messori, J. F. Quinting, J. G. Pinto, and C. M. Grams, "Do atlantic-european weather regimes physically exist?" Geophysical Research Letters **48**, e2021GL095574 (2021).

[13]M. Brunetti, J. Kasparian, and C. Vérard, "Co-existing climate attractors in a coupled aquaplanet," Climate Dynamics **53**, 6293–6308 (2019).

[14]G. Messori and D. Faranda, "Technical note: Characterising and comparing different palaeoclimates with dynamical systems theory," Climate of the Past Discussions (2020).

[15]A. Gualandi, J.-P. Avouac, S. Michel, and D. Faranda, "The predictable chaos of slow earthquakes," Science advances **6**, eaaz5548 (2020).

[16]D. Faranda, M. C. Alvarez-Castro, G. Messori, D. Rodrigues, and P. Yiou, "The hammam effect or how a warm ocean enhances large scale atmospheric predictability," Nature communications **10**, 1–7 (2019).

[17]A. Crisanti, M. Falcioni, A. Vulpiani, and G. Paladin, "Lagrangian chaos: transport, mixing and diffusion in fluids," La Rivista del Nuovo Cimento (1978-1999) **14**, 1–80 (1991).

[18]A. Vulpiani, *Chaos: from simple models to complex systems*, Vol. 17 (World Scientific, 2010).

[19]C. W. Landsea and J. L. Franklin, "Atlantic hurricane database uncertainty and presentation of a new database format," Monthly Weather Review **141**, 3576–3592 (2013).

[20]H. Hersbach, B. Bell, P. Berrisford, S. Hirahara, A. Horányi, J. Muñoz-Sabater, J. Nicolas, C. Peubey, R. Radu, D. Schepers, *et al.*, "The era5 global reanalysis," Quarterly Journal of the Royal Meteorological Society **146**, 1999–2049 (2020).

[21]J. B. Elsner, "Tracking hurricanes," Bulletin of the American Meteorological Society **84**, 353–356 (2003).

[22]J. D. Möller and M. T. Montgomery, "Tropical cyclone evolution via potential vorticity anomalies in a three-dimensional balance model," Journal of the atmospheric sciences **57**, 3366–3387 (2000).

[23]L. J. Shapiro, "Potential vorticity asymmetries and tropical cyclone evolution in a moist three-

layer model," Journal of the atmospheric sciences **57**, 3645–3662 (2000).

[24]L. J. Shapiro and J. L. Franklin, "Potential vorticity in hurricane gloria," Monthly weather review **123**, 1465–1475 (1995).

[25]S. A. Hausman, K. V. Ooyama, and W. H. Schubert, "Potential vorticity structure of simulated hurricanes," Journal of the atmospheric sciences **63**, 87–108 (2006).

[26]K. Tory, N. Davidson, and M. Montgomery, "Prediction and diagnosis of tropical cyclone formation in an nwp system. part iii: Diagnosis of developing and nondeveloping storms," Journal of the atmospheric sciences **64**, 3195–3213 (2007).

[27]T.-Y. Lee, C.-C. Wu, and R. Rios-Berrios, "The role of low-level flow direction on tropical cyclone intensity changes in a moderate-sheared environment," Journal of the Atmospheric Sciences **78**, 2859–2877 (2021).

[28]A. R. Zhai and J. H. Jiang, "Dependence of us hurricane economic loss on maximum wind speed and storm size," Environmental Research Letters **9**, 064019 (2014).

[29]A. C. M. Freitas, J. M. Freitas, and M. Todd, "Hitting time statistics and extreme value theory," Probability Theory and Related Fields **147**, 675–710 (2010).

[30]V. Lucarini, D. Faranda, and J. Wouters, "Universal behaviour of extreme value statistics for selected observables of dynamical systems," Journal of statistical physics **147**, 63–73 (2012).

[31]V. Lucarini, D. Faranda, J. M. M. de Freitas, M. Holland, T. Kuna, M. Nicol, M. Todd, S. Vaienti, *et al.*, *Extremes and recurrence in dynamical systems* (John Wiley & Sons, 2016).

[32]N. R. Moloney, D. Faranda, and Y. Sato, "An overview of the extremal index," Chaos: An Interdisciplinary Journal of Nonlinear Science **29**, 022101 (2019).

[33]M. Süveges, "Likelihood estimation of the extremal index," Extremes **10**, 41–55 (2007).

[34]N. Sarkar and B. B. Chaudhuri, "An efficient differential box-counting approach to compute fractal dimension of image," IEEE Transactions on systems, man, and cybernetics **24**, 115–120 (1994).

[35]F. M. E. Pons, G. Messori, M. C. Alvarez-Castro, and D. Faranda, "Sampling hyperspheres via extreme value theory: implications for measuring attractor dimensions," Journal of statistical physics **179**, 1698–1717 (2020).

[36]D. Faranda and S. Vaienti, "Correlation dimension and phase space contraction via extreme value theory," Chaos: An Interdisciplinary Journal of Nonlinear Science **28**, 041103 (2018).

[37]L.-S. Young, "Dimension, entropy and lyapunov exponents," Ergodic theory and dynamical systems **2**, 109–124 (1982).

[38]L. Pascali, "The wind of change: Maritime technology, trade, and economic development," American Economic Review **107**, 2821–54 (2017).

[39]T. W. Anderson, "On the distribution of the two-sample cramer-von mises criterion," The Annals of Mathematical Statistics , 1148–1159 (1962).

[40]J. Molinari, D. Knight, M. Dickinson, D. Vollaro, and S. Skubis, "Potential vorticity, easterly waves, and eastern pacific tropical cyclogenesis," Monthly weather review **125**, 2699–2708 (1997).

[41]F. Sanders, "Explosive cyclogenesis in the west-central north atlantic ocean, 1981–84. part i: Composite structure and mean behavior," Monthly weather review **114**, 1781–1794 (1986).

[42]R. Klein, "Scale-dependent models for atmospheric flows," Annual review of fluid mechanics **42**, 249–274 (2010).

[43]A. V. Soloviev, R. Lukas, M. A. Donelan, B. K. Haus, and I. Ginis, "Is the state of the air-sea interface a factor in rapid intensification and rapid decline of tropical cyclones?" Journal of Geophysical Research: Oceans **122**, 10174–10183 (2017).

[44]C.-Y. Lee, M. K. Tippett, A. H. Sobel, and S. J. Camargo, "Rapid intensification and the bimodal distribution of tropical cyclone intensity," Nature communications **7**, 1–5 (2016).

[45]M. Ghil, M. D. Chekroun, and E. Simonnet, "Climate dynamics and fluid mechanics: Natural variability and related uncertainties," Physica D: Nonlinear Phenomena **237**, 2111–2126 (2008).

[46]H. A. Dijkstra, *Nonlinear climate dynamics* (Cambridge University Press, 2013).

[47]E.-W. Saw, D. Kuzzay, D. Faranda, A. Guittonneau, F. Daviaud, C. Wiertel-Gasquet, V. Padilla, and B. Dubrulle, "Experimental characterization of extreme events of inertial dissipation in a turbulent swirling flow," Nature communications **7**, 1–8 (2016).

[48]J. Grover and A. Wittig, "Black hole shadows and invariant phase space structures," Physical Review D **96**, 024045 (2017).

[49]F. Bouchet, J. Laurie, and O. Zaboronski, "Langevin dynamics, large deviations and instantons for the quasi-geostrophic model and two-dimensional euler equations," Journal of Statistical Physics **156**, 1066–1092 (2014).

[50]V. Lucarini and T. Bódai, "Edge states in the climate system: exploring global instabilities and critical transitions," Nonlinearity **30**, R32 (2017).

[51]F. Ragone, J. Wouters, and F. Bouchet, "Computation of extreme heat waves in climate models using a large deviation algorithm," Proceedings of the National Academy of Sciences **115**, 24–29 (2018).

[52]D. Faranda, G. Messori, S. Bourdin, M. Vrac, S. Thao, J. Riboldi, S. Fromang, and P. Yiou, "Correcting biases in tropical cyclone intensities in low-resolution datasets using dynamical systems metrics, https://hal.archives-ouvertes.fr/hal-03631098," (2022).

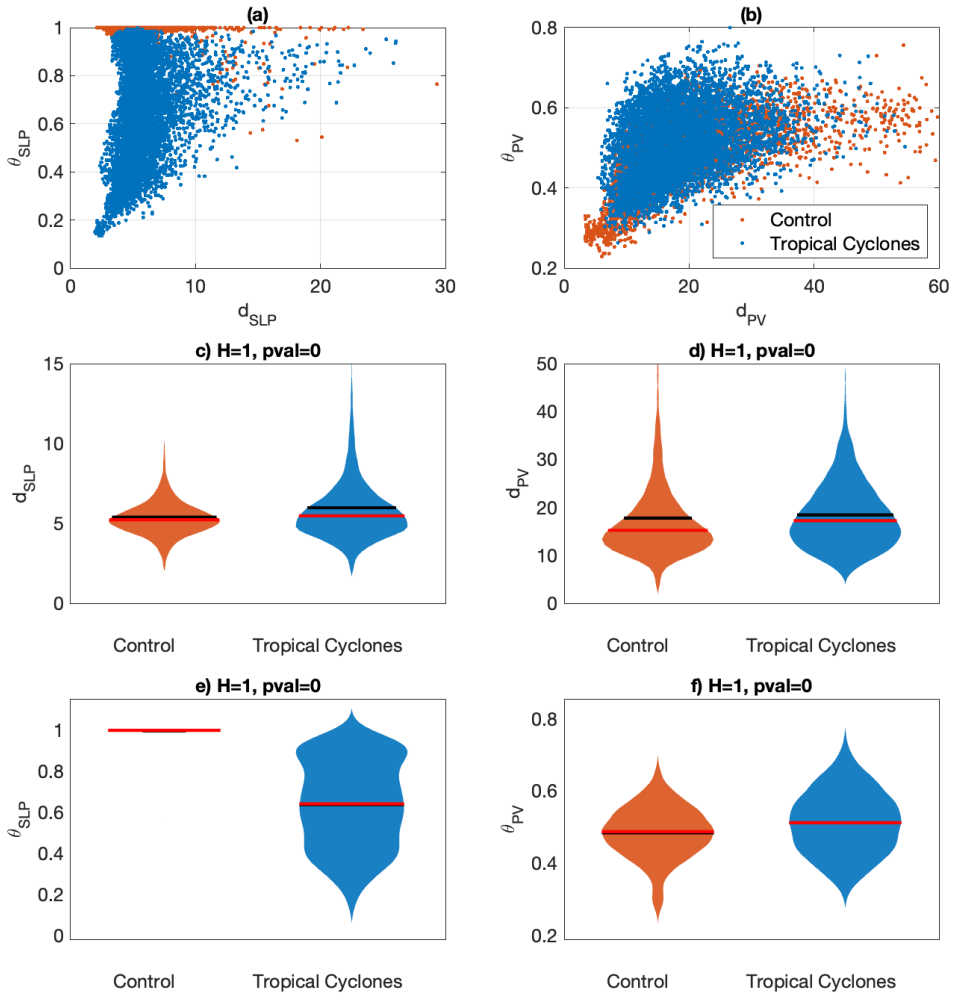

FIG. 2. Dimension d and inverse persistence θ for 6h hourly 2017-2021 ERA5 datasets on a control box [10N<lat<20N -50W<lon<40W] (orange) and for the semilagrangian ERA5 data for tropical cyclones timesteps and center on the cyclones eye coordinates from HURDAT2 database (blue), calculated on sea-level pressure (SLP; a,c,e) and 500 hPa potential vorticity (PV; b, d,f). Panels (a,b) show the dimension-persistence diagrams; panels (c-f) show the violin plots (fatness of the patched area corresponds to the probability density) for the different dataset with the mean (red bars) and the black (medians). Note that the violin plots for the Control box in panel e) are not visible because all values are very close to 1.

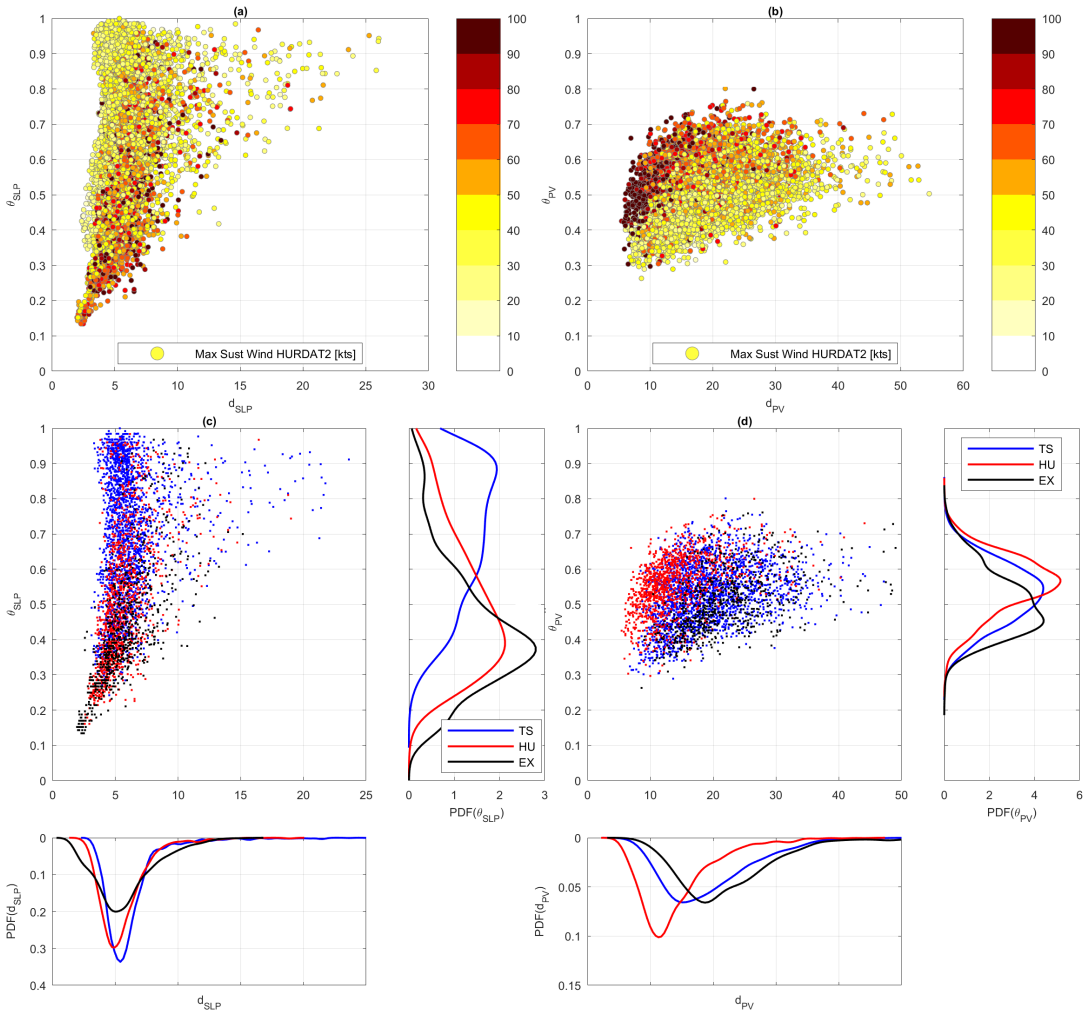

FIG. 3. Dimension d and inverse persistence θ of tropical cyclones, calculated on sea-level pressure (SLP; a,c) and 500 hPa potential vorticity (PV; b, d). The colourscales show maximum wind (a, b) and cyclone classification (c,d, see legend). Side panels show the corresponding PDFs. TS: Tropical Storm; HU: Hurricane; EX: Extratropical cyclones.

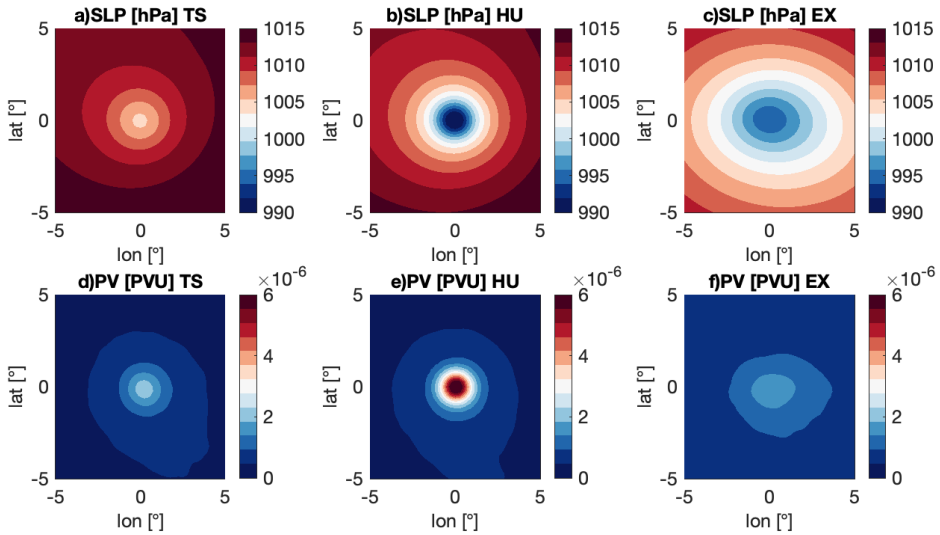

FIG. 4. Average sea-level pressure (SLP, hPa, a–c) and 500 hPa potential vorticity (PV, PVU, d–f) maps conditioned on cyclone classification (TS: Tropical Storm, a,d; HU: Hurricanes, b, e; EX: Extratropical cyclones, c,f).

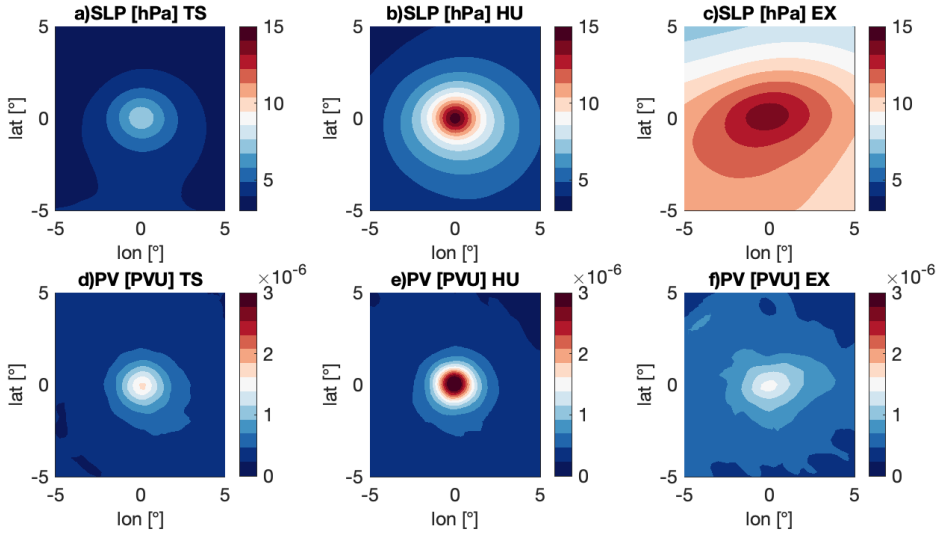

FIG. 5. Same as in Fig. 4, but for the standard deviation of the maps.

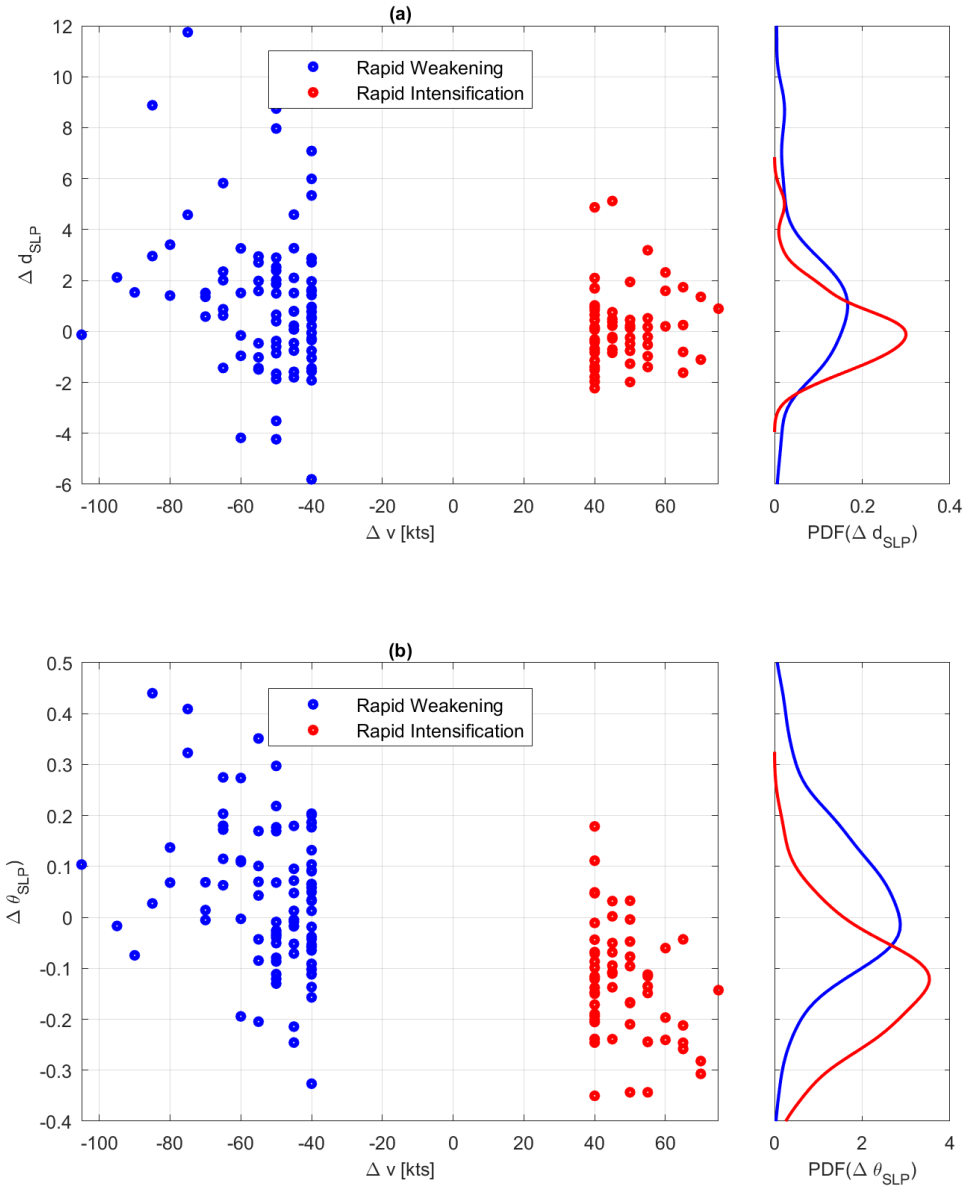

FIG. 6. 24h variation (Δ) of the dimension *d* (a) and of the inverse persistence θ (b) computed on SLP versus the 24h variation of maximum winds *v* for rapidly intensifying (blue) and rapidly weakening (red) cyclones. The side panel shows the corresponding PDFs.

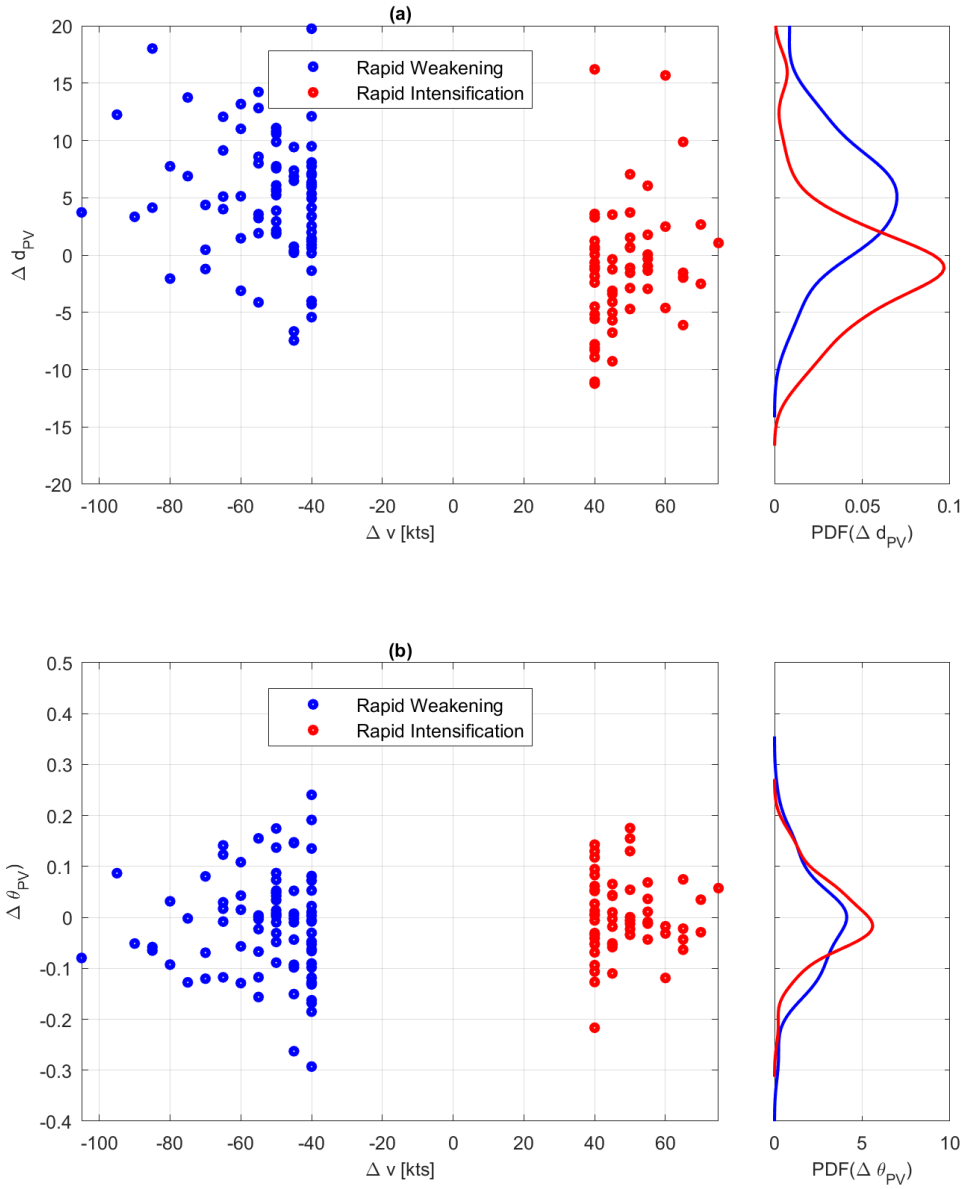

FIG. 7. Same as Fig. 6, but for d and θ computed on PV at 500 hPa.